Inorganic Chemistry

Article

pubs.acs.org/IC

Ambidentate Thiocyanate and Cyanate Ligands in Dinitrosyl Iron Complexes

Chung-Hung Hsieh,[†] Scott M. Brothers,[†] Joseph H. Reibenspies,[†] Michael B. Hall,*[,†] Codrina V. Popescu,*[,‡] and Marcetta Y. Darensbourg*[,†]

[†]Department of Chemistry, Texas A & M University, College Station, Texas 77843, United States

[‡]Department of Chemistry, Ursinus College, Collegeville, Pennsylvania 19426, United States

Supporting Information

ABSTRACT: To explore the effect of delocalization in the $Fe(NO)_2$ unit on possible linkage isomerism of ambidentate ECN^- ligands, E = S and O, anionic DNICs, dinitrosyl iron complexes, $(SCN)_2Fe(NO)_2^-$ (**1**) and $(OCN)_2Fe(NO)_2^-$ (**2**) were synthesized by the reaction of *in situ*-generated $[Fe(CO)_2(NO)_2]^+$ and PPN^+ECN^-. Other $\{Fe(NO)_2\}^9$ (Enemark–Feltham notation) complexes, $(N_3)_2Fe(NO)_2^-$ and $(PhS)_2Fe(NO)_2^-$, were prepared for comparison. The X-ray diffraction analysis of **1** and **2** yielded the typical tetrahedral structures of DNICs with two slightly bent Fe–N–O oriented toward each other, and linear FeNCE units. The ν(NO) IR values shift to lower values for **1** > **2** > $(N_3)_2Fe(NO)_2^-$ > $(PhS)_2Fe(NO)_2^-$, reflecting the increasing donor ability of the ancillary ligands and consistent with the redox potentials of the complexes, and the small trends in Mössbauer isomer shifts. Computational studies corroborate that the $\{Fe(NO)_2\}^9$ motif prefers N-bound rather than E-bound isomers. The calculated energy differences between the linkage isomers of **1** (Fe-NCS preferred over Fe-SCN by about 6 kcal/mol) are smaller than those of **2** (Fe-NCO preferred over Fe-OCN by about 16 kcal/mol), a difference that is justified by the frontier molecular orbitals of the ligands themselves.

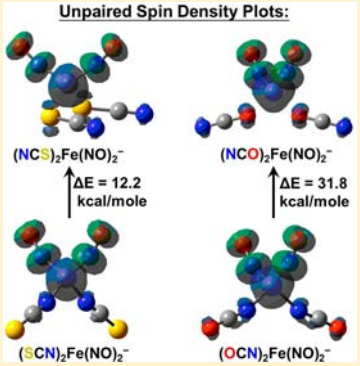

INTRODUCTION

Ambidentate ligands such as thiocyanate, SCN^-, have played important roles in the development of bonding models relating to factors that control linkage isomerism in transition metal complexes.[1] Intensive analyses over decades led to the prospect that ambidentate ligands might serve as a chemical probe for the electronic environment about the metal center, arising both from the oxidation state of the metal as well as the effect of ancillary ligands on the composition of the highest occupied molecular orbital (HOMO) or lowest unoccupied molecular orbital (LUMO).[2] Some early reviews related metal–ligand connectivities to hard (M_{hard}-NCS) and soft (M_{soft}-SCN) bonding patterns, however, and with prescience, these authors noted that intricacies of a steric nature and the influence of supporting ligands might account for deviations from the simple hard/soft interaction expectations.[3,4] In fact, a search of the Cambridge Crystal Structure Data Base from 1990 to current indicates the M-NCS form greatly predominates in almost 500 deposited structures.[1−8] The M-SCN isomer is typical of extreme thiophilic metals such as Hg or Cd, but the M-NCS form is prevalent even in acceptably soft, zerovalent metal carbonyls.[8−10] Interest in the thiocyanates remains high for both fundamental properties and isomerization mechanisms.[1−10] A special application as a photosensitizer, *cis*-$RuL_2(NCS)_2$ (L = 2,2′-bipyridyl-4,4′-dicarboxylic acid), in solar cells has seen continued development.[11−13]

The case of dinitrosyl iron complexes (DNICs) presented herein is particularly intriguing as oxidation state assignments are challenged by the delocalization in the Fe-NO bonds.[14,15] Two redox levels are prevalent for DNICs, represented in the Enemark–Feltham (E-F) notation[16] as $\{Fe(NO)_2\}^9$ and $\{Fe(NO)_2\}^{10}$ for oxidized and reduced levels respectively, each of which have extensive examples in the form of $[X_2Fe(NO)_2]^-$, $[L_2Fe(NO)_2]^0$, and so forth.[17,18] Dimeric and higher aggregates also exist when X^- is a competent bridging ligand such as thiolate sulfur, sulfide, and imidazolate.[19−21] The SCN^- and OCN^- ligands can likewise bind in both monodentate and bridging bonding modes;[1,2] however, to the best of our knowledge, a systematic study of DNICs containing SCN^- and OCN^- ligands, including full characterization and X-ray analysis, is first reported herein.[22]

The E-F notation has circumvented impasses in oxidation state assignments, permitted convenient electron-bookkeeping for redox processes of DNICs, and allowed for a cohesive terminology in the extensive literature regarding DNICs. Recent computations have sought a better understanding of the electronic structure of DNICs isolated in oxidized and reduced redox levels and containing identical supporting Ar-nacnac ligands (Ar-nacnac = anion of [(2,6-diisopropylphenyl)-NC(Me)]$_2$CH).[18,23] While the Fe-NO bond is highly covalent in both, Ye and Neese conclude that oxidized DNIC, $\{Fe(NO)_2\}^9$, is best explained by resonance structures that include high spin ferric (S_{Fe}^{III} = 5/2) and ferrous (S_{Fe}^{II} = 2)

Received: November 19, 2012
Published: February 1, 2013

   dx.doi.org/10.1021/ic3025149 | *Inorg. Chem.* 2013, 52, 2119–2124

antiferromagnetically coupled to triplet NO^- ligands. Reduced $\{Fe(NO)_2\}^{10}$ was more clearly ferrous, with $S_{Fe}^{II} = 2$, again spin coupled to the $^3NO^-$ ligands.[14] The four electrons involved in the three-center FeNO π bonding are generally polarized toward the Fe, so an alternative view would have these four electrons on the Fe but strongly delocalized into the π^* orbitals of NO^+. Still the covalent character of the Fe−N bonds in both redox levels begs the question of whether the iron is to be considered a soft or hard center in terms of ligand bonding in DNICs.

Mononitrosyl iron complexes, especially when porphyrin-based, are known to be of great significance to human physiology. However a similarly important role for DNICs, known to be formed from the degradation of iron−sulfur clusters by excess NO, is controversial.[24−26] Extensive synthetic and reactivity studies have been reported that are likely of import to in vivo mobilization by displacement from protein-bound $(cysteinyl\text{-}S)_2Fe(NO)_2^-$ (high-molecular weight DNICs) by free cysteine or glutathione (producing low molecular weight DNICs).[27] A study of DNICs derived from the intracellular iron pool (CIP) in the presence of glutathione and exogeneous NO conclude such DNICs to have the largest concentration and longest lifetime of all NO-derived cellular adducts.[28,29]

Thiocyanate iron nitrosyl species have been proposed in studies that mimicked conditions resulting from human consumption of iron supplements. The thiocyanate was encountered as a component of saliva while NO was derived from Fe-promoted NO_2^- degradation in the stomach, resulting in ulceration.[30] Despite the paucity of data confirming the nature of such a formulation, and in view of the fundamental inorganic chemistry associated with small molecules as ligands to iron, we report below the synthesis and characterization of bis-triphenylphosphineiminium (PPN^+) salts of $(SCN)_2Fe(NO)_2^-$ (**1**) and $(OCN)_2Fe(NO)_2^-$ (**2**), as well as a unique octahedral ferric thiocyanate, *trans*-$(SCN)_4Fe(THF)_2^-$ (**3**). Characterization by spectroscopies, density functional theory (DFT) analysis, and X-ray diffraction define the nature of the Fe-NCX bonds in the three complexes and compare to related complexes $(N_3)_2Fe(NO)_2^-$ and $(PhS)_2Fe(NO)_2^-$.

EXPERIMENTAL SECTION

General Materials and Techniques. All reactions and operations were carried out on a double-manifold Schlenk vacuum line under N_2 or Ar atmosphere. Tetrahydrofuran (THF), pentane, and diethyl ether were freshly purified by an MBraun Manual Solvent Purification System packed with Alcoa F200 activated alumina desiccant. The purified THF, CH_2Cl_2, pentane, and diethyl ether were stored with molecular sieves under N_2 before experiments. The known complexes $[PPN][Fe(CO)_3(NO)]$,[31] $[PPN][(N_3)_2Fe(NO)_2,]$[19] and $[PPN][(PhS)_2Fe(NO)_2]$ were synthesized by published procedures.[19] The following materials were of reagent grade and were used as purchased from Sigma-Aldrich: sodium thiophenolate, potassium thiocyanate sodium cyanate, and nitrosyl tetrafluoroborate.

Physical Measurements. Infared spectrometry was performed on a Bruker Tensor 27 FTIR spectrometer using 0.1 mm CaF_2 sealed cells. X-band electron paramagnetic resonance (EPR) measurements were obtained on a Bruker EMX spectrometer equipped with ER4102ST cavity and the Oxford Instruments ESR900 cryostat. The microwave frequency was measured with a Hewlett-Packard 5352B electronic counter. Voltammograms were obtained using a standard three-electrode cell under an argon atmosphere at room temperature. Samples in THF were run at a concentration of 2 mM with $[n\text{-}Bu_4N]PF_6$ as the supporting electrolyte (100 mM). Elemental analyses were performed by Atlantic Microlab, inc., Norcross, Georgia, U.S.A.

X-ray Crystal Structure Analyses. A Bausch and Lomb 10× microscope was used to identify suitable crystals of the same habit. Each crystal was coated in paratone, affixed to a Nylon loop and placed under streaming nitrogen (110 K) in a SMART Apex CCD diffractometer (See details in .cif files). The space groups were determined on the basis of systematic absences and intensity statistics. The structures were solved by direct methods and refined by full-matrix least-squares on F^2. Anisotropic displacement parameters were determined for all nonhydrogen atoms. Hydrogen atoms were placed at idealized positions and refined with fixed isotropic displacement parameters. The following is a list of programs used: data collection and cell refinement, APEX2;[32] data reductions, SAINTPLUS Version 6.63;[33] absorption correction, SADABAS;[34] structural solutions, SHELXS-97;[35] structural refinement, SHELXL-97;[36] graphics and publication materials, Mercury Version 2.3.[37]

Mössbauer Measurements. Low-field (0.04 T), variable temperature (4.5−300 K) Mössbauer spectra were recorded on a closed-cycle refrigerator spectrometer, model CCR4K, equipped with a 0.04 T permanent magnet, maintaining temperatures between 4.5−300 K. Mössbauer spectra were analyzed using the software WMOSS (Thomas Kent, SeeCo.us, Edina, Minnesota). The samples were polycrystalline powders, suspended in nujol, placed in Delrin 1.00 mL cups and frozen in liquid nitrogen.

Synthesis of Complex $[PPN][(SCN)_2Fe(NO)_2]$ (1). The $[PPN][Fe(CO)_3(NO)]$ (0.28 g, 0.40 mmol) $[NO]BF_4$ (0.096g, 0.80 mmol) and KSCN (0.078 g, 0.80 mmol) were loaded in a septum-sealed 50 mL Schlenk flask, and 20 mL of THF solvent was added by cannula. The reaction mixture was stirred for overnight at room temperature; its IR spectrum (THF solution) found ν(NO) bands at 1786 (s), 1718 (vs) cm^{-1}. The solution was filtered through Celite to remove insoluble solid. Addition of pentane to the THF solution yielded a brown precipitate, which was washed successively by 1:1 pentane-diethyl ether (3 × 20 mL) to remove impurities (Yield: 0.24 g, 78%). Recrystallization in THF/pentane at −35 °C afforded crystals of complex **1** suitable for X-ray crystallographic study. IR (THF), cm^{-1}: ν(CN) 2076 (sh), 2056 (vs) (SCN); ν(NO) 1786 (s), 1718 (vs). vis−UV, THF solution, nm: 705 (vw), 516 (sh), 399 (m), 292 (sh on intense CT absorption). Elem. anal., found (calc'd for $C_{38}H_{30}FeN_5O_2P_2S_2$) %: C, 59.59 (59.23); H, 3.76 (3.92), N, 8.90 (9.09).

Synthesis of Complex $[PPN][(OCN)_2Fe(NO)_2]$ (2). Following similar procedures as used with complex **1**, $[PPN][Fe(CO)_3(NO)]$ (0.283 g, 0.40 mmol) $[NO]BF_4$ (0.096g, 0.80 mmol) and NaOCN (0.052 g, 0.80 mmol) were loaded in a septum-sealed 50 mL Schlenk flask, and 20 mL of THF solvent was added by cannula and stirred overnight. The solution was filtered through Celite to remove insoluble solid. Complex **2** was isolated as a greenish brown solid after addition of pentane to the THF solution of **2**. (Yield: 0.22g, 75%) Recrystallization in THF/pentane at −35 °C afforded crystals of complex **2** suitable for X-ray crystallographic study. IR (THF), cm^{-1}: ν(CN) 2223 (s), 2197 (vs) (OCN); ν(NO) 1766 (s), 1698 (vs). vis−UV, THF solution, nm: 657 (vw), 508 (m), 375 (sh on intense CT absorption). Elem. anal., found (calc'd for $C_{38}H_{30}FeN_5O_2P_2S_2$) %: C, 62.11 (61.80); H, 4.04 (4.09), N, 9.80 (9.48).

Synthesis of Complex $[PPN][(THF)_2Fe(NCS)_4]$ (3). *Method A.* Complex **1** (0.077g, 0.10 mmol) was dissolved in 20 mL of THF solution in a 100 mL Schlenk flask. Dry air was bubbled into the solution resulting in a color change from brown to red-purple within 20 min. Infrared spectroscopy confirmed reaction completion. The solution was filtered through Celite to remove insoluble solid. After the reaction solution was concentrated to 5 mL, 30 mL of pentane was added to precipitate the product (Yield: 0.030 g, 31%). Layering of THF solution of **3** with a 2:1 mixture of pentane and diethyl ether afforded dark red-purple single crystals after three weeks at −35 °C.

Method B. To a 200 mL Schlenk flask loaded with $FeCl_3{\cdot}6H_2O$ (0.27 g, 1.00 mmol) and PPN^+SCN^- salt (2.33 g, 4.00 mmol), was added 100 mL of THF. The solution was stirred overnight under N_2 and filtered through Celite to remove insoluble solid. Addition of 1:1 pentane-diethyl ether to the THF solution of **3** yielded a dark red-purple precipitate (Yield: 0.86 g, 89%). Elem. anal., found (calc'd for

dx.doi.org/10.1021/ic3025149 | Inorg. Chem. 2013, 52, 2119−2124

$C_{48}H_{46}FeN_5O_2P_2S_4$) %: C, 59.21 (59.38); H, 4.44 (4.78), N, 7.43 (7.21).

RESULTS AND DISCUSSION

As outlined in Scheme 1, the $Fe(CO)_3(NO)^-$ anion is a convenient precursor to $X_2Fe(NO)_2^-$ complexes which makes

Scheme 1. Synthesis of $[PPN][(ECN)_2Fe(NO)_2]$ (E = S and O)

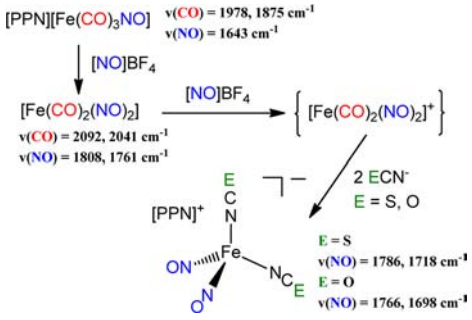

further use of NO^+ as reactant and oxidant converting to an unstable cationic dicarbonyl through the intermediacy of neutral reduced DNIC.[38,39] Anionic ligands readily replace CO and stabilize the $\{Fe(NO)_2\}^9$ unit, as was observed here for SCN^- and OCN^-, complexes **1** and **2**, respectively. This route is also appropriate for formation of $(N_3)_2Fe(NO)_2^-$[19] and $(PhS)_2Fe(NO)_2^-$.

Complexes **1** and **2** were isolated from 1:1 THF/pentane as brown and greenish brown crystals, respectively. The X-ray diffraction analysis yielded the typical tetrahedral structures of DNICs shown in Figure 1; the NCS or NCO ligands are N-

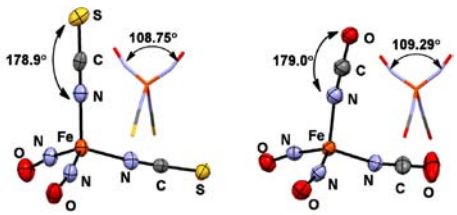

	(SCN)$_2$Fe(NO)$_2^-$ (1)	(OCN)$_2$Fe(NO)$_2^-$ (2)
Fe-NO$_{avg.}$	1.701(2) Å	1.699(2) Å
Fe-NCE$_{avg.}$	1.970(2) Å	1.955(3) Å
N-O$_{avg.}$	1.169(2) Å	1.168(3) Å
Fe-N-O$_{avg.}$	161.9(2)°	161.6(2)°
Fe-N-C$_{avg.}$	177.2(2)°	169.6(3)°
N-C-E$_{avg}$	178.9(2)°	179.0(4) °
ON-Fe-NO	108.75(11)°	109.29(11)°
ECN-Fe-NCE	108.67(9)°	106.39(11)°

Figure 1. Selected metric data are listed below the molecular structures of anionic complexes **1** (E = S) and **2** (E = O), derived from X-ray diffraction analysis of their PPN^+ salts, as thermal ellipsoid plots (50% probability level) with alternate view in capped stick renditions.

bound in both. Differences in the selected metric data given under each structure are largely insignificant, with the largest discrepancy found within the average of Fe−N−C angles (177.2(2)° for **1** and 169.6(3)° for **2**. In both structures the Fe−N−O units are slightly bent, avg. = 162°, and oriented in toward each other. Full metric data for complexes **1** and **2** are provided in Supporting Information, Tables S1 and S2.

For comparison of spectroscopic properties to **1** and **2**, the $(N_3)_2Fe(NO)_2^-$ and $(PhS)_2Fe(NO)_2^-$ complexes were prepared and solution EPR, IR, CV, and solid state Mössbauer spectroscopic studies were carried out. For all, isotropic EPR signals (22 °C in THF solvent), at $g \sim 2.03$, the typical signature for paramagnetic $\{Fe(NO)_2\}^9$ DNICs, were observed with no detectable N-superhyperfine coupling (see Supporting Information, Figure S7). Lippard and co-workers observed that the room temperature EPR spectrum of oxidized N-bound DNIC, (Ar-nacnac)$Fe(NO)_2$ displays an isotropic signal centered at 2.06. The reason(s) for the lack of resolved hyperfine couplings in these complexes is unclear.[18]

The two-band IR spectra in the ν(NO) region are sensitive to ligand,[39] shifting to lower values for **1** > **2** > $(N_3)_2Fe(NO)_2^-$ > $(PhS)_2Fe(NO)_2^-$, Table 1. Note that the $\nu(NO)_{avg.}$ of

Table 1. Mössbauer Parameters: Isomer Shift (δ) and Quadrupole Splitting (ΔE_Q), CV ($E_{1/2}$) and IR Stretching Frequencies of Complexes 1, 2, $(N_3)_2Fe(NO)_2^-$, and $(SPh)_2Fe(NO)_2^-$ and Two Neutral $\{Fe(NO)_2\}^9$ Derivatives for Comparison

	ν(NO)[a] cm^{-1}	$E_{1/2}$[b] (v)	δ[c] (mm/s)	ΔE_Q[c] (mm/s)
	Anionic			
$(SCN)_2Fe(NO)_2^-$	1786, 1718	−1.21	0.35	0.75
$(OCN)_2Fe(NO)_2^-$	1766, 1698	*f.*	0.36	0.70
$(N_3)_2Fe(NO)_2^-$	1755, 1698	−1.51	0.30	0.57
$(PhS)_2Fe(NO)_2^-$	1737, 1693	−1.68	0.23	0.60
	Neutral			
(Ar-nacnac)$Fe(NO)_2$[d]	1761,1709	−1.34	0.19	0.79
(NHC)(PhS)$Fe(NO)_2$[e]	1757, 1712	−1.33	0.15	0.51

[a] THF solution. [b] THF solution, reference to Fc+/Fc. [c] Isomer shifts are quoted at 7 K with respect to Fe metal standard at room temperature. Line-widths are specified in the text. Uncertainties are 0.05 mm/s. [d] See reference 18. [e] See reference 41. [f] Irreversible reduction in THF solution.

$(PhS)_2Fe(NO)_2^-$ is 40 cm^{-1} lower than that of **1**. The trend of increasing electronic donation of X^- (X^- = SCN^-, N_3^-, PhS^-) to the $\{Fe(NO)_2\}^9$ motif is also reflected in the redox potentials of this series of complexes.

The cyclic voltammetry scans of compounds **1**, $(N_3)_2Fe(NO)_2^-$, and $(PhS)_2Fe(NO)_2^-$, measured on 2 mM THF solutions of PPN^+ salts, display one highly reversible electrochemical response within the THF solvent window, Figure 2. The $E_{1/2}$ values are consistent with the ν(NO) IR data, that is, better electron donating ligands render the $\{Fe(NO)_2\}^{9/10}$ couple less accessible.[17,40,41] The CV of the cyanate complex

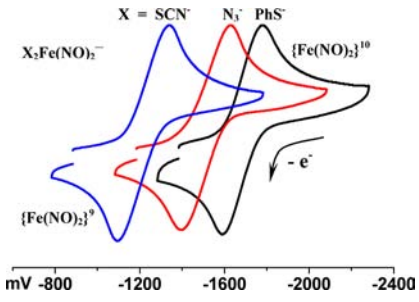

Figure 2. Cyclic voltammograms of complexes **1** (blue; $E_{1/2}$ = −1.21 V), $[PPN][(N_3)_2Fe(NO)_2]$ (red; $E_{1/2}$ = −1.51 V), and $[PPN][(PhS)_2Fe(NO)_2]$ (black; $E_{1/2}$ = −1.68 V) at scan rates 100 mV/s in 2 mM THF solution, referenced to Fc/Fc^+.

dx.doi.org/10.1021/ic3025149 | Inorg. Chem. 2013, 52, 2119−2124

2 shows irreversibility in the analogous redox event, see Supporting Information, Figure S8.

The Mössbauer spectra of the four complexes in an applied field of 0.04 T exhibit broad quadrupole doublets (Supporting Information, Figure S9, fwhm 0.45 mm/s) with no resolved magnetic hyperfine structure, and temperature independent between 5 and 100 K. The 7 K isomer shifts displayed in Table 1 are within the range of high spin Fe(III) complexes.[42] The observed isomer shift for $(PhS)_2Fe(NO)_2^-$ is consistent with published parameters: δ = 0.18 mm/s and ΔE_Q = 0.69 mm/s.[18,20b] For our series of anionic, tetrahedral DNICs the overall trend of δ to smaller values roughly correlates with increasing electron-donating ability of the ancilliary ligand quite reasonably represented by ν(NO) and $E_{1/2}$ values, Table 1.

Also in Table 1 are neutral $\{Fe(NO)_2\}^9$ complexes, that is, with only one anionic ligand, or in case of Ar-nacnac, a monoanionic bidentate ligand, whose IR and $E_{1/2}$ values readily fit into the trend seen for the anionic DNICs. Note however that the Mössbauer isomer shifts do not correlate with the trends in ν(NO) and $E_{1/2}$ values. The overall effect of charge appears to be a factor in the isomer shift data.

Upon exposure to air, the brown color of the THF solution of **1** turns to red-purple, from which X-ray quality crystals were produced on layering with pentane. The molecular structure shown in Figure 3 is that of a monoanionic iron complex of

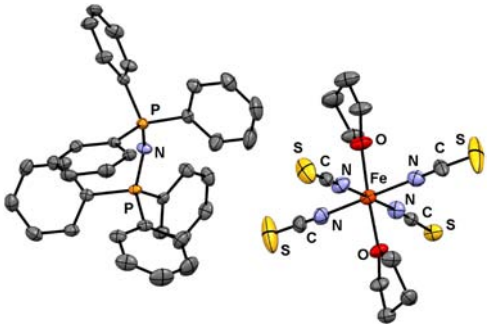

Figure 3. Molecular structure of complex [PPN][$(THF)_2Fe(NCS)_4$] (**3**) as thermal ellipsoid plot (50% probability level). Selected bond distances (Å) and angles (degree): Fe-$NCS_{avg.}$ 2.023(3); Fe−$O(THF)_{avg.}$ 2.089(5); ∠Fe−N−$C_{avg.}$ 171.6.(3); ∠N−C−S_{avg} 178.5(4).. (see Supporting Information, Tables S4 for details of crystallization).

trans-$(THF)_2Fe(NCS)_4^-$ (**3**). This complex is air stable and analogous to the reported *trans*-$(pyridine)_2Fe(NCS)_4^-$.[43] The Gouy balance magnetic susceptibility measurement indicated 5 unpaired electrons, consistent with a high-spin Fe^{III} complex. Complex **3** can also be obtained via reaction of $FeCl_3 \cdot 6H_2O$ and 4 equiv of PPN^+SCN^- salt in THF solution.

Computational Studies. The molecular structures of the ligands N_3^-, OCN^-, and SCN^-, as well as the corresponding DNICs, $(N_3)_2Fe(NO)_2^-$, $(NCS)_2Fe(NO)_2^-$ (**1**), and $(NCO)_2Fe(NO)_2^-$ (**2**), have been optimized and analyzed by DFT computations using a methodology previously determined to be accurate for DNICs: the BP86 functional[44,45] and a mixed basis set of SDD ECP on Fe and 6-311++G(d,p)[46−49] on all other atoms.[50] See Supporting Information for details. The O-bound and S-bound linkage isomers of the latter two complexes have also been investigated. In all cases, the N-bound derivatives were found as the ground state, consistent with experiment; linkage isomerism from N to S requires approximately 6 kcal/mol per SCN^- ligand and from N to O requires approximately 16 kcal/mol per OCN^- ligand. The unpaired spin density plot, Supporting Information, Figure S11 and TOC graphic, shows that the unpaired density is confined to the $Fe(NO)_2$ unit.

The preference for N-binding over O or S is found in the ligands themselves. The frontier molecular orbitals of OCN^-, specifically the π (HOMO) and σ (HOMO-1) orbitals, both have primarily N-character, see Figure 4. The SCN^- ligand also

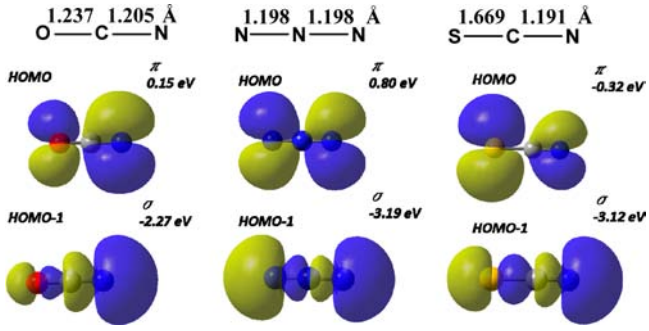

Figure 4. Selected Frontier Molecular Orbitals (FMOs), orbital character, and orbital energies (eV) of the triatomic ligands OCN^-, N_3^-, and SCN^-. Molecular orbital contours plotted at an isosurface value of 0.02 au. Internal distances given for triatomic anions are from computer optimized structures.

donates through the π (HOMO) and σ (HOMO-1) orbitals; however, the former has significant S-character, while the latter retains substantial N-character. Both OCN^- and SCN^- are expected to have contributions from both the E=C=N$^-$ and the $^-$E−C≡N resonance structures, with the latter structure contributing more in SCN^-. That this resonance structure is more important in SCN^- leads to the greater linearity of the Fe−N=C angle of complex **1** vs **2**, see Supporting Information.

Since the NO ligands in the iron dinitrosyl unit are very strong π-acceptors, the ancillary ligands should be expected to bind in a manner that would yield the better σ donations. Thus, the preferred SCN^- and OCN^- derivatives are bound through the N. The competition between the S π vs N σ donation is responsible for the ambidenticity of the SCN^- ligand and for the relatively small isomerism energy in **1**, while the OCN^- ligand with both σ and π donor orbitals on N shows a much larger isomerism energy in **2**. Further, the π-donation when S-bound results in a strongly bent SCN^- linkage (average Fe−S−C angle of 107.2°), while the σ-donation resulting from N-binding produces a nearly linear linkage (average Fe−N=C angle of 169.4°), which is the structural form found in our studies.

The influence of the other ligands with respect to the linkage isomerism of SCN^- has been further explored by investigation of the carbonyl derivatives of the Fe^0 and Fe^{II} compounds: $Fe(CO)_4(NCS)^-$ and $(\eta^5\text{-}C_5H_5)Fe(CO)_2(NCS)$, see Figure 5. These complexes have ΔE between N- and S-bound SCN^- ligands of 2.82 and 1.08 kcal/mol respectively, consistent with the decrease in the π-acceptor strength of the other ligands, that is, CO and Cp. The known experimental isomers provide confirmation of this conclusion, as $Fe(CO)_4(NCS)^-$ has been crystallized in only the N-bound form,[51] whereas both N- and S-bound isomers of $(\eta\text{-}C_5H_5)Fe(CO)_2(NCS)$ have been separated by chromatography and isolated.[52]

dx.doi.org/10.1021/ic3025149 | *Inorg. Chem.* 2013, 52, 2119−2124

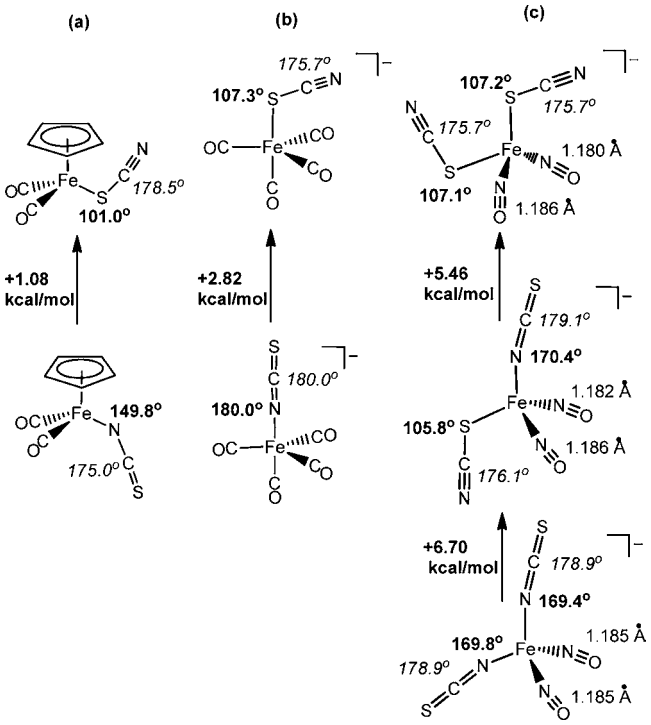

Figure 5. Calculated isomers and electronic energy differences of (a) $(Cp)Fe(CO)_2(NCS)$, (b) $Fe(CO)_4(NCS)^-$, and (c) $Fe(NO)_2(NCS)_2^-$. Angles given in italics represent the SCN bond angle, and angles given in bold font represent the Fe–N/S–C bond angle.

The ν(NO) IR stretching frequencies of complex **1** (1786 s, 1718 vs cm^{-1}) are among the highest of isolated anionic $\{Fe(NO)_2\}^9$ DNICs.[48,40,53,54] This is significant in terms of NO-releasing activity as it has been established that higher ν(NO) values of DNICs correlate with ease of NO transfer to NO-trapping agents. The SCN^- and OCN^- DNICs are also informative as to the regulation of the electronic environment possible by ancillary ligands of the $Fe(NO)_2$ fragment. Such fine-tuning behavior of the $Fe(NO)_2$ fragment is noted in both ν(NO) and $E_{1/2}$ values. However, oxidation state assignments, in attempts to define the $Fe(NO)_2$ unit "beyond the E-F notation",[55] cannot be based on IR and cyclic voltammetry. Determination of Fe and NO redox levels require detailed interpretation of Mössbauer and computational data, and other advanced spectroscopic techniques.

■ ASSOCIATED CONTENT

Ⓢ Supporting Information

X-ray crystallographic data (CIF) from the structure determinations, ORTEPs, and full lists of metric parameters for complexes **1**–**3**. EPR spectra of complexes **1** and **2**. Cyclic voltammogram of complex **2**. Computational metric data and APT population analysis for complexes **1**, **2**, $[PPN][(N_3)_2Fe(NO)_2]$, and $[PPN][(PhS)_2Fe(NO)_2]$. Calculated isomers and electronic energy differences of **1** and **2**. Unpaired spin density plots for the $\{Fe(NO)_2\}^9$ isomers of **1** and **2**. Frontier molecular orbitals (FMOs) of the iron fragments $Fe(NO)_2^+$, $(Cp)Fe(CO)_2^+$, and $Fe(CO)_4$. FMOs of the complexes $(CO)_4Fe(SCN)^-$, $(CO)_4Fe(NCS)^-$, $(Cp)Fe(CO)_2(SCN)$, and $(Cp)Fe(CO)_2(NCS)$. FMOs of the complexes $(OCN)_2Fe(NO)_2^-$, $(NCO)_2Fe(NO)_2^-$, $(SCN)_2Fe(NO)_2^-$, and $(NCS)_2Fe(NO)_2^-$. This material is available free of charge via the Internet at http://pubs.acs.org.

■ AUTHOR INFORMATION

Corresponding Author

*E-mail: marcetta@mail.chem.tamu.edu (M.Y.D.), hall@chem.tamu.edu (M.B.H.), cpopescu@ursinus.edu (C.V.P.).

Notes

The authors declare no competing financial interest.

■ ACKNOWLEDGMENTS

We are grateful for financial support from the National Science Foundation (CHE-0910679 to MYD, CHE-0956779 to CVP, and CHE-0910552 to MBH) and the R. A. Welch Foundation (A-0924 to MYD and A-0648 to MBH).

■ REFERENCES

(1) Burmeister, J. L. *Coord. Chem. Rev.* **1966**, *7*, 205–221.
(2) Burmeister, J. L. Newman, A. A., Ed.; Academic Press: London, U.K., 1975; pp 68–130.
(3) Gray, H. B.; Gutterman, D. F. *J. Am. Chem. Soc.* **1971**, *93*, 3364–3371.
(4) Gray, H. B.; Gutterman, D. F. *Inorg. Chem.* **1972**, *11*, 1727–1733.
(5) Pohl, K.; Wieghardt, K.; Nuber, B.; Weiss, J. *J. Chem. Soc., Dalton Trans.* **1987**, 187–192.
(6) Maroney, M. J.; Fey, E. O.; Baldwin, D. A.; Stenkamp, R. E.; Jensen, L. H.; Rose, N. J. *Inorg. Chem.* **1986**, *25*, 1409–1414.
(7) Brewster, T. P.; Ding, W.; Schley, N. D.; Hazari, N.; Batista, V. S.; Crabtree, R. H. *Inorg. Chem.* **2011**, *50*, 11938–11946.
(8) Kuang, S.-M.; Xue, F.; Duan, C.-Y.; Mak, T. C.W.; Zhang, Z.-Z. *J. Organomet. Chem.* **1997**, *534*, 15–21.
(9) Sloan, T. E.; Wojcicki, A. *Inorg. Chem.* **1968**, *7*, 1268–1273.
(10) Berndt, A. F.; Barnett, K. W. *J. Organomet. Chem.* **1980**, *184*, 211–219.
(11) Nazeeruddin, M. K.; Péchy, P.; Renouard, T.; Zakeeruddin, S. M.; Humphry-Baker, R.; Comte, P.; Liska, P.; Cevey, L.; Costa, E.; Shklover, V.; Spiccia, L.; Beacon, G. B.; Bignozzi, C. A.; Grätzel, M. *J. Am. Chem. Soc.* **2001**, *123*, 1613–1624.
(12) Mosconi, E.; Yum, J.-H.; Kessler, F.; Gomez-Garcia, C. J.; Zuccaccia, C.; Cinti, A.; Nazeeruddin, M. K.; Grätzel, M.; De Angelis, F. *J. Am. Chem. Soc.* **2012**, *134* (47), 19438–19453.
(13) Brown, D. G.; Sanguantrakun, N.; Schulze, B.; Schubert, U. S.; Berlinguette, C. P. *J. Am. Chem. Soc.* **2012**, *134*, 12354–12357.
(14) Ye, S.; Neese, F. *J. Am. Chem. Soc.* **2010**, *132*, 3646–3647.
(15) Yeh, S.-W.; Lin, C.-W.; Li, Y.-W.; Hsu, I.-J.; Chen, C.-H.; Jang, L.-Y.; Lee, J.-F.; Liaw, W.-F. *Inorg. Chem.* **2012**, *51*, 4076–4087.
(16) Enemark, J. H.; Feltham, R. D. *Coord. Chem. Rev.* **1974**, *13*, 339–406.
(17) Hsieh, C.-H.; Darensbourg, M. Y. *J. Am. Chem. Soc.* **2010**, *132*, 14118–14125.
(18) (a) Harrop, T. C.; Tonzetich, Z. J.; Reisner, E.; Lippard, S. J. *J. Am. Chem. Soc.* **2008**, *130*, 15602–15610. (b) Tonzetich, Z. J.; Do, L. H.; Lippard, S. J. *J. Am. Chem. Soc.* **2009**, *131*, 7964–7965.
(19) Tsai, M.-L.; Hsieh, C.-H.; Liaw, W.-F. *Inorg. Chem.* **2007**, *46*, 5110–5117.
(20) (a) Chiang, C. Y.; Miller, M. L.; Reibenspies, J. H.; Darensbourg, M. Y. *J. Am. Chem. Soc.* **2004**, *126*, 10867–10874. (b) Hess, J. L.; Hsieh, C.-H.; Brothers, S. M.; Hall, M. B.; Darensbourg, M. Y. *J. Am. Chem. Soc.* **2011**, *133*, 20426–20434.
(21) Wang, X.; Sundberg, E. B.; Li, L.; Kantardjieff, K. A.; Herron, S. R.; Lim, M.; Ford, P. C. *Chem. Commun.* **2005**, 477–479.
(22) Bryar, T. R.; Eaton, D. R. *Can. J. Chem.* **1992**, *70*, 1917–1926.
(23) Tonzetich, Z. J.; Héroguel, F.; Do, L. H.; Lippard, S. J. *Inorg. Chem.* **2011**, *50*, 1570–1579.
(24) Foster, M. W.; Cowan, J. A. *J. Am. Chem. Soc.* **1999**, *121*, 4093–4100.

dx.doi.org/10.1021/ic3025149 | *Inorg. Chem.* 2013, 52, 2119–2124

(25) (a) Ding, H.; Demple, B. *Proc. Natl. Acad. Sci. U.S.A.* **2000**, *97*, 5146−5150. (b) Yang, W.; Rogers, P. A.; Ding, H. *J. Biol. Chem.* **2002**, *277*, 12868−12873.
(26) Tran, C. T.; Kim, E. *Inorg. Chem.* **2012**, *51*, 10086−10088.
(27) (a) Vanin, A. F.; Mikoyan, V. D.; Kubrina, L. H. *Mol. Biophys.* **2010**, *55*, 5−12. (b) Burgova, E. N.; Adamyan, L. V.; Tkachev, N. A.; Stepanyan, A. A.; Vanin, A. F. *Biophysics* **2012**, *57*, 87−89.
(28) Hickok, J. R.; Sahni, S.; Shen, H.; Arvind, A.; Antoniou, C.; Fung, L. W.M.; Thomas, D. D. *Free Radical Biol. Med.* **2011**, *51*, 1558−1566.
(29) Rahmanto, Y. S.; Kalinowski, D. S.; Lane, D. R.; Lok, H. C.; Richardson, V.; Richardson, D. R. *J. Biol. Chem.* **2012**, *287*, 6960−6968.
(30) Takahama, U.; Hirota, S. *Chem. Res. Toxicol.* **2012**, *25*, 207−215.
(31) Hedberg, L.; Hedberg, K.; Satija, S. K.; Swanson, B. I. *Inorg. Chem.* **1985**, *24*, 2766.
(32) *APEX2*, version 2009.7-0; Bruker AXS, Inc.: Madison, WI, 2007.
(33) *SAINTPLUS: Program for Reduction of Area Detector Data*, 1034 version 6.63; Bruker AXS Inc.: Madison, WI, 2007.
(34) Sheldrick, G. M. *SADABS: Program for Absorption Correction of 1036 Area Detector Frames*; Bruker AXS Inc.: Madison, WI, 2001.
(35) Sheldrick, G. M. *SHELXS-97: Program for Crystal Structure 1038 Solution*; Universität Göttingen: Göttingen, Germany, 1997.
(36) Sheldrick, G. M. *SHELXL-97: Program for Crystal Structure 1040 Refinement*; Universität Göttingen: Göttingen, Germany, 1997.
(37) Macrae, C. F.; Edgington, P. R.; McCabe, P.; Pidcock, E.; 1042 Shields, G. P.; Taylor, R.; Towler, M.; van de Streek, J. *J. Appl. Crystallogr.* **2006**, *39*, 453−457.
(38) Tsai, M.-C.; Tsai, F.-T.; Lu, T.-T.; Tsai, M.-L.; Wei, Y.-C.; Hsu, I.-J.; Lee, J.-F.; Liaw, W.-F. *Inorg. Chem.* **2009**, *48*, 9579−9591.
(39) Klein, A.; Mering, Y.; Uthe, A.; Butsch, K.; Schaniel, D.; Mockus, N.; Woike, T. *Polyhedron* **2010**, *29*, 2553−2559.
(40) Tsai, F.-T.; Chiou, S.-J.; Tsai, M.-C.; Tsai, M.-L.; Huang, H.-W.; Chiang, M.-H.; Liaw, W.-F. *Inorg. Chem.* **2005**, *44*, 5872−5881.
(41) Hess, J. L.; Hsieh, C.-H.; Reibenspies, J. H.; Darensbourg, M. Y. *Inorg. Chem.* **2011**, *50*, 8541−8552.
(42) Stefanikova, S.; Ondrejkovicova, I.; Koman, M.; Lis, T.; Mrozinski, J.; Wrzecion, M. *J. Coord. Chem.* **2008**, *61*, 3895−3903.
(43) Drago, R. S. *Physical Methods for Chemists*, 2nd ed.; Saunders College Pub.: Ft. Worth, TX, 1992.
(44) Becke, A. D. *Phys. Rev. A* **1988**, *38*, 3098−3100.
(45) Perdew, J. P. *Phys. Rev. B* **1986**, *33*, 8822−8824.
(46) Krishnan, R.; Binkley, J. S.; Seeger, R.; Pople, J. A. *J. Chem. Phys.* **1980**, *72*, 650.
(47) Wachters, A. J. H. *J. Chem. Phys.* **1970**, *52*, 1033.
(48) Hay, P. J. *J. Chem. Phys.* **1977**, *66*, 4377−4384.
(49) Raghavachari, K.; Trucks, G. W. *J. Chem. Phys.* **1989**, *91*, 1062−1065.
(50) Brothers, S. M.; Darensbourg, M. Y.; Hall, M. B. *Inorg. Chem.* **2011**, *50*, 8532−8540.
(51) Ruff, J. K. *Inorg. Chem.* **1969**, *8*, 86−89.
(52) Sloan, T. E.; Wojcicki, A. *Inorg. Chem.* **1968**, *7*, 1268−1273.
(53) Schmidt, J. *Transition Met. Chem.* **1979**, *1*, 256−259.
(54) Roncaroli, F.; ve Eldik, R.; Olabe, J. A. *Inorg. Chem.* **2005**, *44*, 2781−2790.
(55) Tomson, N. C.; Crimmin, M. R.; Petrenko, T.; Rosebrugh, L. E.; Sproules, S.; Boyd, W. C.; Bergman, R. G.; DeBeer, S.; Toste, F. D.; Wieghardt, K. *J. Am. Chem. Soc.* **2011**, *133*, 18785−18801.

dx.doi.org/10.1021/ic3025149 | *Inorg. Chem.* 2013, 52, 2119−2124